

Resonant Raman scattering and the zone-folded electronic structure in single-wall nanotubes

A. Kasuya and M. Sugano

Institute for Materials Research, Tohoku University, Sendai 980-77, Japan

T. Maeda

Department of Basic Science, Ishinomaki Senshu University, Ishinomaki 986, Japan

Y. Saito

Department of Electrical and Electronic Engineering, Mie University, Tsu 514, Japan

K. Tohji and H. Takahashi

Department of Geoscience and Technology, Tohoku University, Sendai 980-77, Japan

Y. Sasaki, M. Fukushima, Y. Nishina, and C. Horie

Department of Basic Science, Ishinomaki Senshu University, Ishinomaki 986, Japan

(Received 14 July 1997; revised manuscript received 27 October 1997)

Resonant Raman scattering from optical phonons in single-wall nanotubes of mean diameter 1.1 nm has been measured for incident laser beams with wavelength between 450 and 800 nm. The scattering intensities exhibit anomalies in the vicinity of 690 nm, there being a minimum in the longitudinal components and a maximum in the transverse. Our optical-transmission measurement also exhibits a dip in the same photon energy range. The anomalies are caused by the incident laser beam resonant with the zone-folded electronic structures in nanotubes. These results provide direct experimental evidence of the critical point in the density of states produced by the cylindrical symmetry of nanotubes. [S0163-1829(98)10209-6]

Many distinctive features of nanotubes have been predicted in the zone-folding effect of their dispersion relations based on graphite.¹⁻³ The effect arises from their cylindrical symmetry and causes drastic modifications in their material properties as a result of the unique nanometer scale system. The zone-folding effect in the electronic states induces one-dimensional $E^{-1/2}$ singularities in the density of states at energies where corresponding wave vectors k_n , along the circumference direction become equal to the inverse of the tube radius, and its integer multiples, $k_n = n/r$ ($n = 1, 2, \dots$). Many of these critical points lie in the energy range of 1 eV and may play decisive roles in the electronic as well as optical properties of nanotubes derived from graphite. It is, therefore, essential to identify and characterize the low-lying electronic states in understanding the basic size-dependent properties of nanotubes.

This paper presents an experimental evidence on such critical point structures in the electronic states found in our resonant Raman-scattering and optical-absorption spectra. The recent Raman-scattering measurements on single-wall nanotubes show evidence for the zone-folding effect in the phonon system.^{4,5} The diameter selected samples allowed us to determine the diameter-dependent phonon dispersion in the multiple splittings of the optical phonon peak measured with the incident beam of an Ar ion laser at 514.5 nm.⁴ As the wavelength increases, the Raman-scattering intensities exhibit anomalies in the vicinity of 690 nm. The optical absorption spectrum also shows a dip in the same range of wavelength. The Raman scattering from graphite, on the other hand, shows only a monotonous decrease in the intensity due to the decrease in the density of states from the

π -band contribution in the measured range from 450 to 800 nm. These experimental results provide a direct evidence in the presence of the critical point structure produced by the zone-folding effect in nanotubes.

Samples are prepared by arc discharging of graphite electrodes in He gas of pressure 600 Torr, as described previously.⁶ The positive electrode is filled with Fe and Ni powders of equal atomic weight in the center. Our electron microscopic observation indicates that our samples contain more than 20% of single-wall nanotubes of mean diameter 1.1 nm. The diameter distribution is rather narrow and the mean deviation is less than ± 0.1 nm.⁶ The Raman scattering is measured in a back scattering geometry at room temperature with a single monochromator connected to a liquid-nitrogen-cooled charge-coupled device camera. Ar ion laser together with a dye laser and a Ti-sapphire laser are used as excitation sources.

Figure 1 shows our Raman-scattering spectra of optical phonons centered at 1580 cm^{-1} measured with the incident laser of wavelength from 488 to 783 nm. Spectra show multiply split peaks and shoulders on the both sides of the graphite peak at 1580 cm^{-1} that is displayed at the top in Fig. 1. These split peaks and shoulders correspond to longitudinal (LO) and transverse (TO) modes branched off from the Γ point to higher and lower energies, respectively, with discrete wavevectors k_n in the graphite dispersion. The intensity of LO is much higher than those of TO. As the wavelength increases from 488 to 690 nm, however, the former becomes comparable to the latter, and then increases again as the wavelength increases further towards 800 nm. The observation of these two types of wavelength dependencies is con-

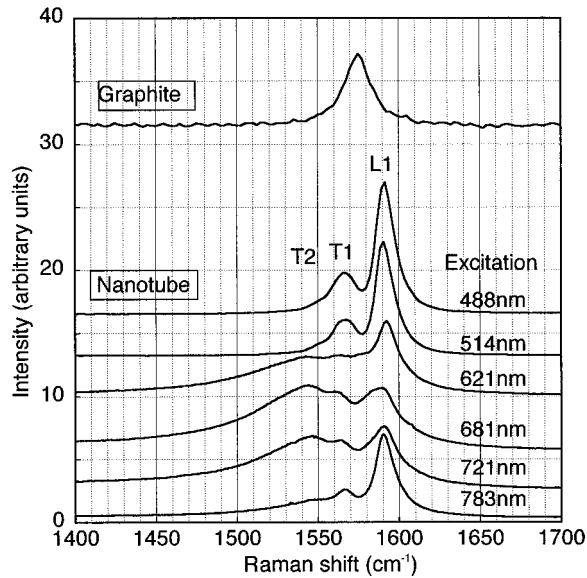


FIG. 1. Raman-scattering spectra between 1400 and 1700 cm^{-1} from single-wall nanotubes of diameter 1.1 nm excited by the incident laser of wavelengths from 488 to 783 nm. The top spectrum is from graphite (highly oriented pyrolytic graphite) excited at 488 nm.

sistent with our interpretation⁴ that the splittings are grouped into two components of LO and TO, which exhibit different electron-phonon couplings in the Raman-scattering process. The peak at 1590.9 cm^{-1} is denoted as L1, and peaks at 1567.5 and 1549.2 cm^{-1} are marked as T1 and T2, respectively, in Fig. 1. The numbers 1 and 2 refer to the subscript of k_n ($n=1,2$) zone-folded onto the Γ point.

Figure 2 is a plot of Raman peak intensities for L1, T1, and T2 vs the wavelength of incident laser beam. Also plotted is the intensity of graphite peak at 1580 cm^{-1} . The Raman peaks show a minimum for L1 and a maximum for T1 and T2 at a nearly equal wavelength of incident laser beam in the vicinity of 690 nm. The intensity of T2 increases more than T1 and all three peaks become comparable at the extreme. The intensity of graphite at 1580 cm^{-1} , on the other hand, decreases monotonously with increasing wavelength and shows no particular anomaly.

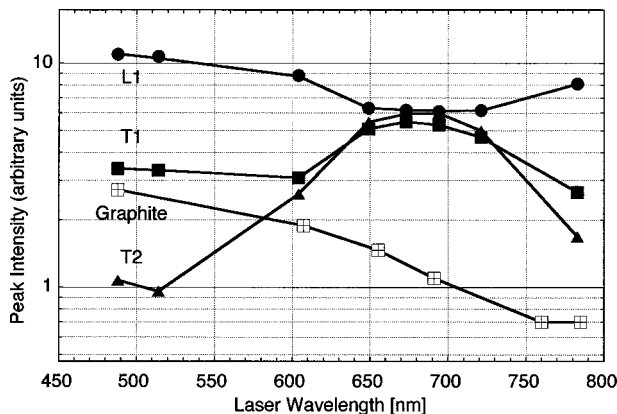


FIG. 2. Variations of Raman peak intensity for L1, T1, and T2 and graphite in the incident wavelength range between 488 and 783 nm.

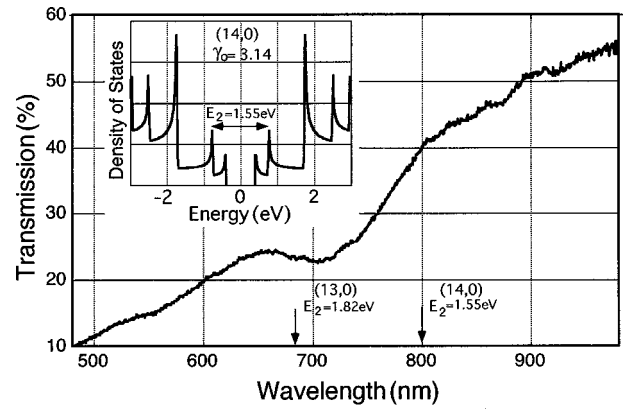


FIG. 3. Optical transmission spectrum in nanotubes measured in the wavelength region from 480 to 980 nm. The inset shows the density of states calculated for the tube with diameter 1.096 nm of type (14,0), the zigzag tube with 14 hexagons around the circumference. The band parameter $\gamma_0=3.14$.

Figure 3 shows an optical transmission spectrum of our sample in the wavelength ranging from 480 to 980 nm. It shows a dip near 710 nm below the background contribution which increases monotonously with increasing wavelength up to 480 nm. This background contribution is explained by the density of states in the continuous π bands in graphite. It is well investigated both experimentally and theoretically that the density of states in the π band of graphite increases smoothly with increasing energy up to the first critical point at the Q point in the two-dimensional Brillouin zone (corresponding to the LM line in the three-dimensional zone). Any sharp structure, therefore, is attributed to the density of states structure originated from the symmetry change of nanotube with respect to graphite.

In the zone-folding scheme, the electronic state of nanotubes consists of a set of one-dimensional bands having continuous values of the wavevectors along the cylindrical axis of the tube but is discrete in the circumference direction of wavevectors equal to k_n . Each band exhibits $E^{-1/2}$ singularity in the density of states at the band edge. Hence, the sum of density of states shows a series of $E^{-1/2}$ singularities with each superposed on top of continua composed of the tails of other $E^{-1/2}$ singularities. The inset in Fig. 3 shows an example calculated for the tube with diameter 1.096 nm that is nearly equal to 1.1 nm of our samples. The tube type is (14,0), the zigzag tube with 14 hexagons around the circumference. The energy band is obtained in the tight-binding approximation with $\gamma_0=3.14$, energy of the nearest-neighbor C-C overlapping integral.^{3,7}

According to the calculation, the energy separation, E_1 between the pair of singularities nearest from the Fermi energy ($=0$) is 0.76 eV, and E_2 , the next nearest is 1.55 eV for $\gamma_0=3.14$. In Fig. 3, E_2 for (14,0) is marked together with (13,0) of diameter 1.026 nm at 1.82 eV. For the armchair tube with diameter 1.079 nm of type (8,8), $E_1=1.58$ eV for $\gamma_0=2.5$ estimated by a local density-functional calculation.^{5,7} These values of E_1 and E_2 lie in the energy range of the dip centered at 1.75 eV (710 nm) in the optical transmission spectrum in Fig. 3. Corresponding values of diameters also lie in the range of 1.1 ± 0.1 nm of our electron microscopic observation. Hence, the dip found in our trans-

mission measurement is accounted well by the $E^{-1/2}$ singularities produced by the zone-folding effect.

In addition to the main dip centered at 710 nm, Fig. 3 shows smaller but sharper dips at many spectral positions in the transmission such as around 920, 870, and 550 nm as well as within the main dip. Their depths vary independently of each other from position to position of our measurements on the sample. Figure 3 represents a typical spectrum. This variation comes from the spatial inhomogeneity of nanotube types in our sample. The observed behavior together with the above critical point calculation indicate that the main dip in the spectrum is superpositions of many sharper dips contributed from major types of nanotubes in the diameter range of 1.1 ± 0.1 nm. More precise band-structure information on graphite, especially for γ_0 , specifies further the tube types of our samples and the locations of zone-folded bands.

In interpreting our Raman-scattering measurement, one may note that the incident laser beam is resonant with the direct electronic transition in both nanotubes and graphite. The scattering cross section depends sensitively on the critical point structure in the energy bands of resonance. Hence, the observed anomalies shown in Fig. 2 provides a direct evidence of critical points in the energy region of our measurement. These critical points are produced by the zone-folding effect because the graphite do not show such anomalies in our measurement as shown in Fig. 2. The presence of these critical points are also proved directly in our optical transmission measurement that exhibits a dip at a nearly equal spectral position and width as compared with the anomalies in the Raman intensity. The width of the anomaly

lies is explained by the diameter and chiral angle distributions.

The anomalies found in Fig. 2 exhibit a minimum for LO and a maximum for TO. This resonant behavior implies a complicated critical point structure in the density of states of nanotubes. In the zone-folded electronic bands, the sharp $E^{-1/2}$ singularity is superposed on continuous tails of other bands. The resonant scattering contributions via these discrete and continuous states may cancel each other through a Fano-type interference,⁸ leading to a decrease in the total Raman-scattering cross section in LO.

The destructive interference effect has been found in resonant Raman scatterings from the phonon system in many semiconductors, such as Si, CdS, and ZnS, with the incident photon energy at the fundamental edge or in higher conduction bands where the scattering contributions from critical points of different types and dimensions overlapped with the continuous background.⁹⁻¹¹ The enhancement is observed both from LO and TO but the cancellation has been found only for TO. The cancellation for LO is found in ZnO.¹²

In summary, our resonant Raman-scattering spectrum shows anomaly in the wavelength range of incident laser beam in the vicinity of 690 nm. This anomaly not present in graphite comes from singularities in the electronic density of states produced by the zone-folding effect in nanotubes. The presence of critical points is also shown consistently in our optical absorption measurements.

This work was supported by CREST of Japan Science and Technology Institute.

¹N. Hamada, S. Sawada, and A. Oshiyama, Phys. Rev. Lett. **68**, 1579 (1992).

²R. Saito, M. Fujita, G. Dresselhaus, and M. S. Dresselhaus, Appl. Phys. Lett. **60**, 2204 (1992).

³R. A. Jishi, D. Inomata, K. Nakao, M. S. Dresselhaus, and G. Dresselhaus, J. Phys. Soc. Jpn. **63**, 2252 (1994).

⁴A. Kasuya, Y. Sasaki, Y. Saito, K. Tohji, and Y. Nishina, Phys. Rev. Lett. **78**, 4434 (1997).

⁵A. M. Rao *et al.*, Science **275**, 187 (1997).

⁶Y. Saito, M. Okuda, and T. Koyama, Surf. Rev. Lett. **3**, 863 (1996).

⁷J. W. Mintmire and C. T. White, Carbon **33**, 893 (1995).

⁸U. Fano, Phys. Rev. **124**, 1866 (1961).

⁹J. M. Ralston, R. L. Wadsack, and R. K. Chang, Phys. Rev. Lett. **25**, 814 (1970).

¹⁰T. C. Damen and J. F. Scott, Solid State Commun. **9**, 383 (1971).

¹¹*Light Scattering in Solids*, edited by M. Balkanski (Flammarion Sciences, Paris, 1971), p. 43.

¹²R. H. Callender, S. S. Sussman, M. Selders, and R. K. Chang, Phys. Rev. B **7**, 3788 (1973).